Heat and Mass Transfer 39 (2003) 305–312
DOI 10.1007/s00231-002-0353-4

Thermal radiation effects on MHD forced convection flow adjacent to a non-isothermal wedge in the presence of a heat source or sink

Ali J. Chamkha, Mir Mujtaba, A. Quadri, Camille Issa

Abstract This work is focused on the steady-state, hydromagnetic forced convective boundary-layer flow of an incompressible Newtonian, electrically-conducting and heat-generating/absorbing fluid over a non-isothermal wedge in the presence of thermal radiation effects. The wedge surface is assumed permeable so as to allow for possible wall suction or injection. Also included in the model are the effects of viscous dissipation, Joule heating and stress work. The governing partial differential equations for this investigation are derived and transformed using a non-similarity transformation. In deriving the governing equations, a temperature-dependent heat source or sink term is employed and the Rossland approximation for the thermal radiation term is assumed to be valid. The obtained non-similar equations are solved numerically by an implicit, iterative, tri-diagonal finite-difference method. Comparisons with previously published work on various special cases of the problem are performed and the results are found to be in excellent agreement. Numerical results for the velocity and temperature profiles for a prescribed magnetic parameter as well as the development of the local skin-friction coefficient and local Nusselt number with the magnetic parameter are presented graphically and discussed. This is done in order to elucidate the influence of the various parameters involved in the problem on the solution.

Nomenclature

A positive constant defined in Eqs. (4)
B_o externally imposed magnetic field in the y-direction
c_p specific heat at constant pressure
C positive constant defined in Eqs. (4)
C_f local skin-friction coefficient, $2\nu(\partial u/\partial y)_{y=0}/U_\infty^2$
Ec Eckert number, $U_\infty^2/\{c_p[T_w(x) - T_\infty]\}$
f dimensionless stream function, defined in Eqs. (8)
f_o wall mass transfer parameter
k thermal conductivity
K mean radiation absorption coefficient
m pressure gradient parameter, $\beta/(2 - \beta)$
N_R thermal radiation parameter defined in Eqs. (11)
Nu_x local Nusselt number, defined in Eqs. (13b)
Pr Prandtl number, ν/α
q_r radiative heat flux defined by Eq. (5)
Q_o heat generation or absorption coefficient
Re_x local Reynolds number, $U_\infty x/\nu$
T temperature
u velocity component in the x-direction
U_∞ potential flow or free stream velocity, Cx^m
v velocity component in the y-direction
v_o suction (>0) or injection (<0) velocity
x coordinate along the wedge surface
y coordinate normal to the wedge surface

Greek Symbols

α thermal diffusivity
β angle factor of the wedge
η pseudosimilarity variable, defined in Eqs. (8)
ξ magnetic variable, in Eqs. (8)
Ω total angle of the wedge
ϕ dimensionless heat generation or absorption coefficient defined in Eqs. (11)
θ dimensionless temperature, defined in Eqs. (8)
ρ density of fluid
ν kinematic viscosity
σ electrical conductivity
σ^* Stefan-Boltzmann constant
ψ stream function

Subscripts

w condition at the wall
∞ condition at free stream

Received: 19 April 2001
Published online: 13 March 2003

A.J. Chamkha (✉), M. Mujtaba, A. Quadri
Department of Mechanical Engineering, Kuwait University,
P.O. Box 5969, Safat, 13060 – Kuwait
E-mail: chamkha@kuc01.kuniv.edu.kw

C. Issa
Department of Civil Engineering,
Lebanese American University, Byblos, Lebanon

1 Introduction

Lately, hydromagnetic flow and heat transfer problems have become more important in many engineering and industrial applications. These include Magnetohydrodynamic power generators and accelerators, cooling of nuclear reactors, and crystal growth. As a result, a significant amount of research has been carried out on the effects of electrically-conducting fluids such as liquid metals, water mixed with a little acid and others in the presence of a magnetic field on the flow and heat transfer aspects from various geometries. For example, Michiyoshi et al. (1976) have considered natural convection heat transfer from a horizontal cylinder to mercury under a magnetic field. Gray (1979) has studied laminar wall plume in a transverse magnetic field. Fumizawa (1980) has reported a natural convection experiment with liquid NaK under a transverse magnetic field. Vajravelu and Nayfeh (1992) have studied hydromagnetic convection at a cone and a wedge. Chamkha (1997a) has analyzed hydromagnetic natural convection from an isothermal inclined surface adjacent to a thermally stratified porous medium. Recently, Yih (1999) has considered MHD forced convection flow adjacent to a non-isothermal wedge in the presence of viscous and magnetic dissipations and stress work.

In many situations, there may be an appreciable temperature difference between the surface and the ambient fluid. This necessitates the consideration of temperature-dependent heat sources or sinks which may exert strong influence on the heat transfer characteristics. The study of heat generation or absorption in moving fluids is important in view of several physical problems such as fluids undergoing exothermic or endothermic chemical reactions (see Vajravelu and Hadjinicolaou, 1993 and Vajravelu and Nayfeh, 1992). In addition, natural convection with heat generation can be applied to combustion modelling (Westphal et al., 1994). Although, exact modelling of the internal heat generation or absorption is quite difficult, some simple mathematical models can express its average behavior for most physical situations. Heat generation or absorption has been assumed to be constant, space-dependent or tempearature dependent. Sparrow and Cess (1961) have considered temperature dependent heat absorption in their work on steady stagnation point flow and heat transfer. Moalem (1976) has studied the effect of temperature-dependent heat sources taking place in electrical heating on the heat transfer within a porous medium. Vajravelu and Nayfeh (1992) have reported on the hydromagnetic convection at a cone and a wedge in the presence of temperature-dependent heat generation or absorption effects. Recently, Chamkha (1997b) has considered linear variation with temperature dependent heat sources or sinks in his work on mixed convection in a channel filled with a porous medium. Finally, Crepeau and Clarksean (1997) have used a space-dependent exponentially decaying heat generation or absorption model in their work on flow and heat transfer from a vertical plate.

The role of thermal radiation on flow and heat transfer processes is of major importance in the design of many advanced energy conversion systems operating at high temperature. Thermal radiation within these systems is usually the result of emission by the hot walls and the working fluid. Raptis (1998a) has considered thermal radiation effects on flow of micropolar fluids past a continuously moving plate. Raptis (1998b) has analyzed thermal radiation and free convection flow through a porous medium.

The objective of this paper is to generalize the work of Yih (1999) by including the effects of wall blowing or suction, temperature-dependent heat generation or absorption and thermal radiation effects. This will be done for power-law variation of the wall temperature.

2
Governing equations:

Consider steady, laminar, two dimensional hydromagnetic boundary-layer flow and heat transfer over a permeable non-isothermal wedge in the presence of thermal radiation and heat generation or absorption effects. Fluid suction or injection is imposed at the surface of the wedge. The applied magnetic field is assumed to be uniform and is in the direction normal to the surface. All fluid properties are assumed to be constant and the magnetic Reynolds number is assumed to be small so that the induced magnetic field can be neglected. The latter assumption uncouples the Navier–Stokes from Maxwell's equations (see, Cramer and Pai, 1973). No electric field is assumed to exist and the Hall effect is negligible. The effects of viscous dissipation, Joule heating, and the stress work are included in the present work. The equations governing this boundary-layer forced convection flow situation are based on the balance laws of mass, linear momentum, and energy. These can be written as

$$\frac{\partial u}{\partial x} + \frac{\partial v}{\partial y} = 0 \tag{1}$$

$$u\frac{\partial u}{\partial x} + v\frac{\partial u}{\partial y} = \nu\frac{\partial^2 u}{\partial y^2} + U_\infty\frac{dU_\infty}{dx} + \frac{\sigma B_o^2}{\rho}(U_\infty - u) \tag{2}$$

$$u\frac{\partial T}{\partial x} + v\frac{\partial T}{\partial y} = \alpha\frac{\partial^2 T}{\partial y^2} + \frac{Q_o}{\rho c_p}(T - T_\infty) + \frac{1}{\rho c_p}\frac{\partial q_r}{\partial y} + \frac{\nu}{c_p}\left(\frac{\partial u}{\partial y}\right)^2 - \frac{u}{c_p}\left(U_\infty\frac{dU_\infty}{dx} + \frac{\sigma B_o^2}{\rho}U_\infty\right) + \frac{\sigma B_o^2 u^2}{\rho c_p} \tag{3}$$

The physics of the problem suggests the following boundary conditions

$$\begin{aligned} &y = 0: \quad u = 0,\ v = -v_o,\ T = T_w(x) = T_\infty + Ax^{2m} \\ &y \to \infty: \quad u \to U_\infty = Cx^m,\ T \to T_\infty \end{aligned} \tag{4}$$

where x and y are coordinates measured along and normal to the surface, respectively. u and v are the velocity components in the x and y directions, respectively. ν is the kinematic viscosity. $U_\infty = Cx^m$ is the free stream velocity of the potential flow outside the boundary layer, $m = \beta/(2 - \beta)$, and β is the Hartree pressure gradient parameter which corresponds to $\beta = \Omega/\pi$ for a total angle of the wedge. C is a positive number. σ is the electrical conductivity. B_o is the externally imposed magnetic field in the y-direction. ρ is the density. T is the temperature. α is the thermal diffusivity. c_p is the specific heat at constant pressure. A is a positive number. Q_o is the heat generation

(>0) or absorption (<0) coefficient, q_r is the radiative heat flux. v_o is the suction (>0) or injection(<0) velocity. T_∞ is the free stream temperature.

In addition, the radiative heat flux q_r is employed according to Rosseland approximation such that

$$q_r = -\frac{4\sigma^*}{3K}\frac{\partial T^4}{\partial y} \tag{5}$$

where σ^* and K are the Stefan-Boltzmann constant and the mean absorption coefficient, respectively. As done by Raptis (1998a, b), the fluid-phase temperature differences within the flow are assumed to be sufficiently small so that T^4 may be expressed as a linear function of temperature. This is done by expanding T^4 in a Taylor series about the free stream temperature T_∞ and neglecting higher-order terms to yield

$$T^4 = 4T_\infty^3 T - 3T_\infty^4 \tag{6}$$

By using Equations (5) and (6) in Equation (3), one obtains

$$\begin{aligned} u\frac{\partial T}{\partial x} + v\frac{\partial T}{\partial y} &= \alpha\frac{\partial^2 T}{\partial y^2} + \frac{Q_o}{\rho c_p}(T - T_\infty) \\ &\quad - \frac{16\sigma^* T_\infty^3}{3K\rho c_p}\frac{\partial^2 T}{\partial y^2} + \frac{v}{c_p}\left(\frac{\partial u}{\partial y}\right)^2 \\ &\quad - \frac{u}{c_p}\left(U_\infty\frac{dU_\infty}{dx} + \frac{\sigma B_o^2}{\rho}U_\infty\right) + \frac{\sigma B_o^2 u^2}{\rho c_p} \end{aligned} \tag{7}$$

Defining the stream function in the usual way such that $u = \partial\psi/\partial y$ and $v = -\partial\psi/\partial x$ and substituting the following dimensionless variables

$$\begin{aligned} &\xi = \frac{\sigma B_o^2 x}{\rho U_\infty}, \quad \eta = \frac{y}{x}\left(\frac{U_\infty x}{v}\right)^{1/2} \\ &f(\xi,\eta) = \frac{\psi}{(U_\infty x v)^{1/2}}, \quad \theta(\xi,\eta) = \frac{T - T_\infty}{T_w - T_\infty} \end{aligned} \tag{8}$$

into Equations (1), (2) and (7) results in the following non-similar equations:

$$\begin{aligned} &f''' + \left(\frac{1+m}{2}\right)ff'' + m[1 - (f')^2] + \xi(1 - f') \\ &\quad = (1-m)\xi\left(f'\frac{\partial f'}{\partial \xi} - f''\frac{\partial f}{\partial \xi}\right) \end{aligned} \tag{9}$$

$$\begin{aligned} &\frac{(1+N_R)}{\Pr}\theta'' + \left(\frac{1+m}{2}\right)f\theta' - 2mf'\theta + \phi\xi\theta \\ &\quad + Ec[(f'')^2 - (m+\xi)f' + \xi(f')^2] \\ &\qquad = (1-m)\xi\left(f'\frac{\partial \theta}{\partial \xi} - \theta'\frac{\partial f}{\partial \xi}\right) \end{aligned} \tag{10}$$

where

$$\begin{aligned} &\Pr = \frac{v}{\alpha}, \quad N_R = \frac{16\sigma^* T_\infty^3}{3Kk}, \quad \phi = \frac{Q_o}{\sigma c_p B_o^2} \\ &Ec = \frac{U_\infty^2}{c_p(T_w - T_\infty)} = \frac{C}{c_p A} \end{aligned} \tag{11}$$

are the Prandtl number, thermal radiation parameter, dimensionless heat generation or absorption coefficient, and the Eckert number, respectively.

The dimensionless form of the boundary conditions become

$$\begin{aligned} &\eta = 0: \quad f' = 0, \; f = \left(\frac{2}{1+m}\right)f_o\xi^{1/2}, \; \theta = 1 \\ &\eta \to \infty: \quad f' \to 1, \; \theta \to 0 \end{aligned} \tag{12}$$

where $f_o = (\rho/(v\sigma B_o{}^2))^{1/2} v_o$ is the dimensionless suction or injection parameter such that $f_o>0$ indicates wall suction and $f_o<0$ indicates wall injection or blowing.

Equations (9) and (10) have the property of becoming self similar at $\xi=0$ and therefore, generates their own starting profiles for the numerical computations. In addition, it is also observed that for m=1 (linear free stream velocity with axial distance) these equations become similar for any specific value of ξ.

Important physical parameters for this flow and heat transfer situation are the local skin-friction coefficient and the local Nusselt number. These are defined as follows:

$$\begin{aligned} &C_f = \frac{\mu\,\partial u/\partial y|_{y=0}}{1/2\rho U_\infty v/x} = 2\mathrm{Re}_x^{1/2} f''(\xi,0) \\ &Nu_x = \frac{-k\,\partial T/\partial y|_{y=0}}{k(T_w - T_\infty)/x} = -\mathrm{Re}_x^{1/2}\theta'(\xi,0) \end{aligned} \tag{13}$$

where $\mathrm{Re}_x = U_\infty x/v$ is the local Reynolds number

3 Numerical method

Equations (9) through (12) represent an initial-value problem with ξ playing the role of time. This problem is non-linear and possesses no analytical solution. Therefore, it must be solved numerically. The implicit finite-difference method discussed by Blottner (1970) is chosen for this purpose because it has been proven to be adequate and to give accurate results for boundary-layer equations.

All first-order derivatives with respect to ξ are replaced by two-point backward difference formulae of the form

$$\frac{\partial A}{\partial \xi} = \frac{A_{m,n} - A_{m-1,n}}{\Delta\xi} \tag{14}$$

where A is any dependent variable and m and n are node locations along the ξ and η directions, respectively. The third-order differential equation (9) is converted into a second-order one by substituting V = f′. Then all second order equations for V and θ are discretized using three-point central difference quotients while the first order differential equation governing f is discretized by the trapezoidal rule. At each line of constant ξ, a set of algebraic equations results. With the non-linear terms evaluated at the previous iteration, the algebraic equations are solved with iteration by the well known Thomas algorithm (see Blottner, 1970). The same process is repeated for the next ξ value and the problem is solved line by line until the desired ξ value is reached. A convergence criterion based on the relative difference between the current and the previous iterations is employed. When this difference

Table 1. Comparison of the values of $f'(0, 0)$ for various values of m with $f_o = 0$

m	Cebeci and Bradshaw (1984)	Yih (1999)	Present results
−0.05	0.21351	0.213484	0.213802
0.0	0.33206	0.332057	0.332206
1/3	0.75745	0.757448	0.757586
1.0	1.23259	1.232588	1.232710

Table 2. Comparison of the values of $f''(\xi, 0)$ for m = 1 with $f_o = 0$

ξ	Sparrow et al. (1962)	Ariel (1994)	Yih (1999)	Present results
0	1.231	1.232588	1.232588	1.232710
1	1.584	1.585331	1.585331	1.585480
4	2.345	2.346663	2.346663	2.341002
9	–	3.240950	3.240950	3.240992
25	–	5.147965	5.147964	5.148002
100	–	10.074741	10.074741	10.075001

Table 3. Comparison of the values of $-\theta'(0,0)$ for various values of Pr with $Ec = f_o = m = N_R = \phi = 0$

Pr	Lin and Lin (1987)	Yih (1999)	Present results
0.0001	0.005588	0.005590	0.005670
0.001	0.017316	0.017316	0.017381
0.01	0.051590	0.051589	0.051830
0.1	0.140032	0.140034	0.142003
1	0.332057	0.332057	0.332173
10	0.728148	0.728141	0.72831
100	1.57186	1.571831	1.57218
1000	3.38710	3.387083	3.38809
10000	7.29742	7.297402	7.30080

reaches 10^{-5}, the solution is assumed converged and the iteration process is terminated. A representative set of numerical results is shown graphically in Figures 1 through 12, to illustrate the influence of various parameters on the velocity and temperature profiles. The accuracy of the numerical method was checked by performing various comparisons at different conditions with previously published work. These comparisons are shown in

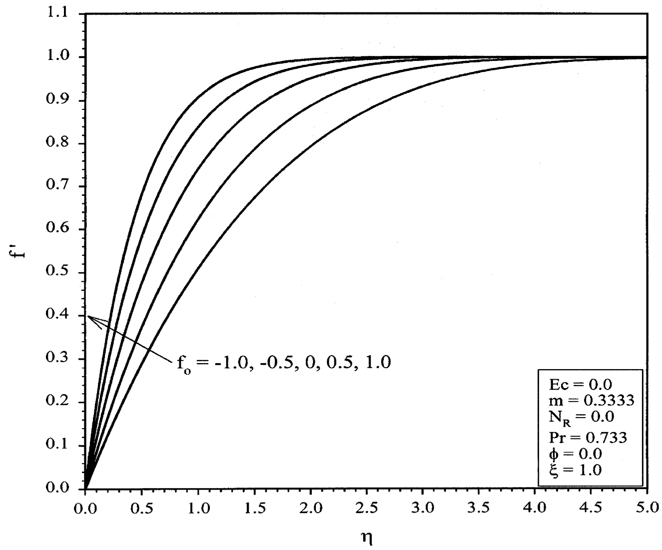

Fig. 1. Effects of f_o on Velocity Profiles

Tables 1 through 4. As obvious from these tables, excellent agreement between the results exists. These favorable comparisons lend confidence in the numerical method employed and the numerical results to be presented subsequently.

4
Results and discussion

Figures 1 and 2 present representative velocity and temperature profiles at the magnetic parameter $\xi = 1.0$ for various values of the dimensionless suction or injection parameter (or wall mass transfer parameter) f_o. Imposition of wall fluid suction ($f_o>0$) has the tendency to reduce both the hydrodynamic and thermal boundary layers resulting in increases in the fluid velocity and decreases in the fluid temperature. On the other hand the exact opposite effect occurs when wall fluid injection is imposed. These behaviors are evident from Figures 1 and 2.

In Figures 3 and 4, the effects of f_o on the development of both the local skin-friction coefficient ($0.5C_fRe_x^{1/2}$) and the local Nusselt number ($Nu_xRe_x^{-1/2}$) with the magnetic parameter ξ are displayed. Inspection of Figures 1 and 2 reveals that the wall slopes of the velocity and temperature

Table 4 Comparison of the values of $-\theta(\xi, 0)$ for vaious values of Pr and Ec with $f_o = m = N_R = \phi = 0$

		Watanabe and Pop (1994)		Yih (1999)		Present results	
Pr	ξ	Ec = 0	Ec = 1	Ec = 0	Ec = 1	Ec = 0	Ec = 1
0.733	0.0	0.29755	0.12395	0.297526	0.170272	0.297600	0.170184
	0.5	0.35699	0.20871	0.357022	0.210072	0.357040	0.209858
	1.0	0.38336	0.22857	0.382588	0.228813	0.383191	0.229000
	1.5	0.39959	0.24122	0.398264	0.240798	0.399980	0.241002
	2.0	0.41091	0.25022	0.409168	0.249316	0.409450	0.249307
1	0.0	0.33206	0.16603	0.332057	0.166029	0.332173	0.166302
	0.5	0.40280	0.20144	0.402864	0.201452	0.403103	0.201630
	1.0	0.43446	0.21727	0.433607	0.216814	0.433901	0.216721
	1.5	0.45413	0.22710	0.452634	0.226323	0.452808	0.226213
	2.0	0.46798	0.23401	0.465987	0.232998	0.466111	0.233102

profiles increase and decrease, respectively as f_o increases. Therefore, according to Equations (13), this causes the values of both the local skin-friction coefficient and the local Nusselt number to increase as f_o increases as is evident from Figures 3 and 4. It is also observed from these figures that the skin-friction coefficient increases with ξ for all values of f_o considered except in the immediate vicinity of the cone apex (or no magnetic field) at $\xi=0$ where $0.5C_fRe_x^{1/2}$ decreases slightly. The Nusselt number is predicted to increase with ξ for values of $f_o \geq 0$ and to decrease for values of $f_o<0$ (injection).

Figures 5 through 8 illustrate the influence of the free stream velocity (or pressure gradient) parameter m on the velocity and temperature profiles at $\xi=1.0$ as well as the development of both the local skin-friction coefficient and local Nusselt number with ξ, respectively. As the parameter m increases, both the velocity and temperature are predicted to decrease. This is accompanied by an increase in the hydrodynamic boundary layer and a decrease in the thermal boundary layer as shown in Figures 5 and 6. The wall slopes of the velocity and temperature profiles are both observed to decrease resulting in decreases and increases in the local skin-friction coefficient and local Nusselt number, respectively. Since f_o is taken to be zero in obtaining Figures 5 through 8, both $0.5C_fRe_x^{1/2}$ and $Nu_x Re_x^{-1/2}$ increase with increasing values of ξ.

Figures 9 and 10 depict the effects of the thermal radiation parameter N_R on the temperature profile (at $\xi=1.0$) and the development of the local Nusselt number with ξ, respectively. Increases in the values of N_R have the tendency to increase the conduction effect and to increase the thermal boundary layer. This, in turn, causes the temperature to increase at every point away from the wedge surface. Since the wall slope of the temperature profile

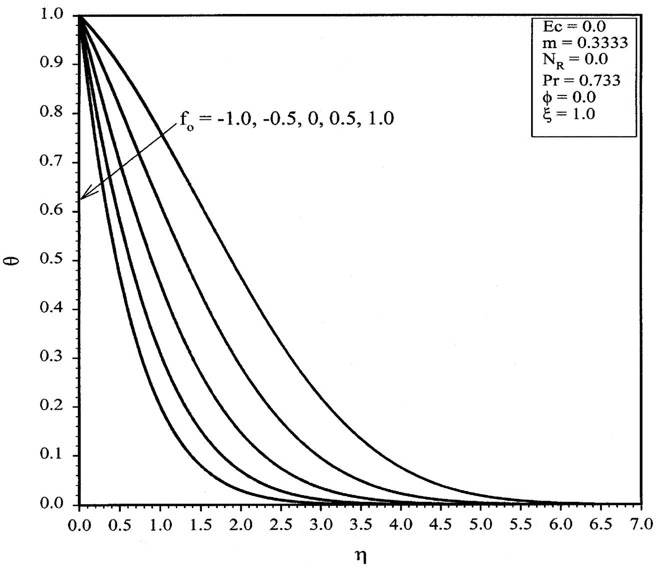

Fig. 2. Effects of f_o on Temperature Profiles

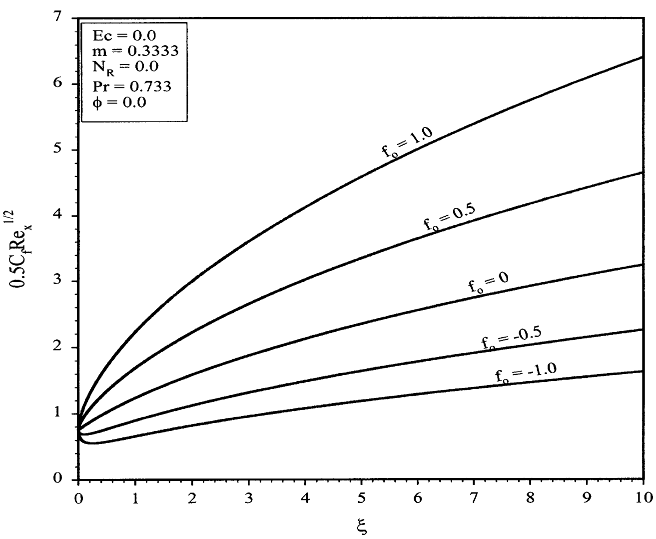

Fig. 3. Effects of f_o on Development of Skin-Friction Coefficient

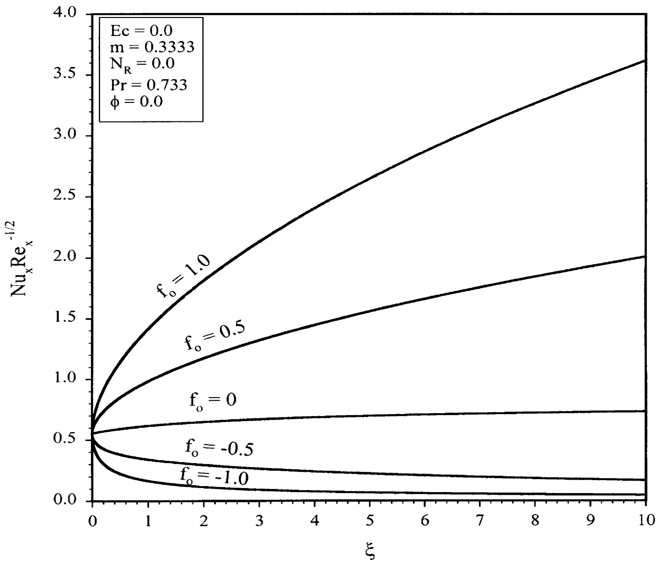

Fig. 4. Effects of f_o on Development of Nusselt Number

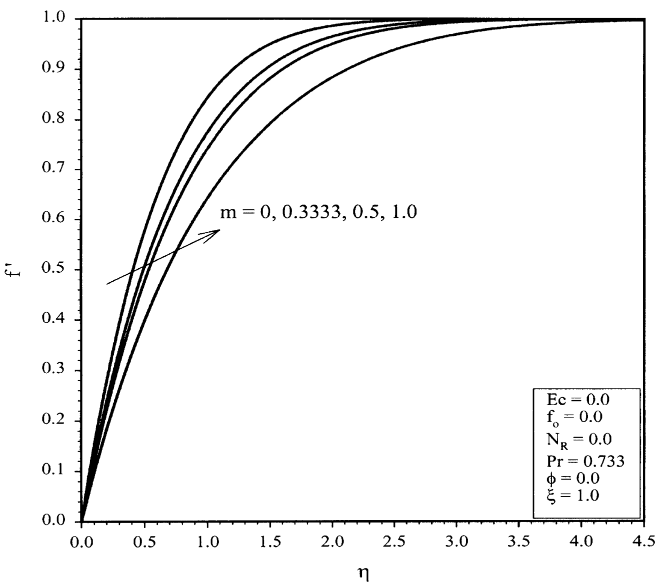

Fig. 5. Effects of m on Velocity Profiles

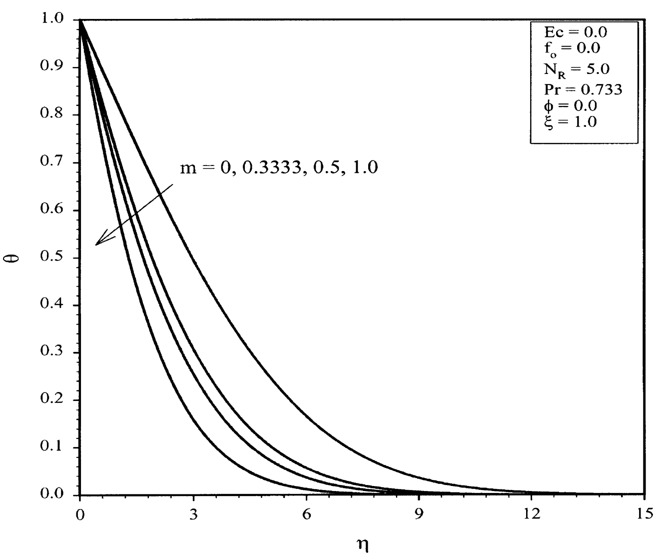

Fig. 6. Effects of m on Temperature Profiles

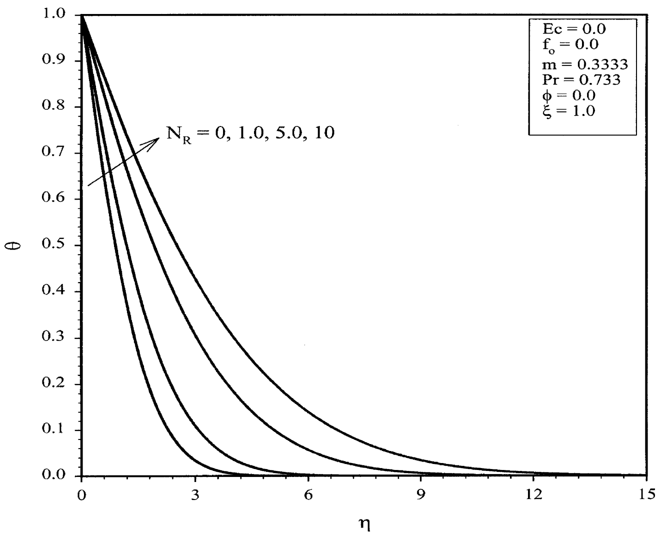

Fig. 9. Effects of N_R on Temperature Profiles

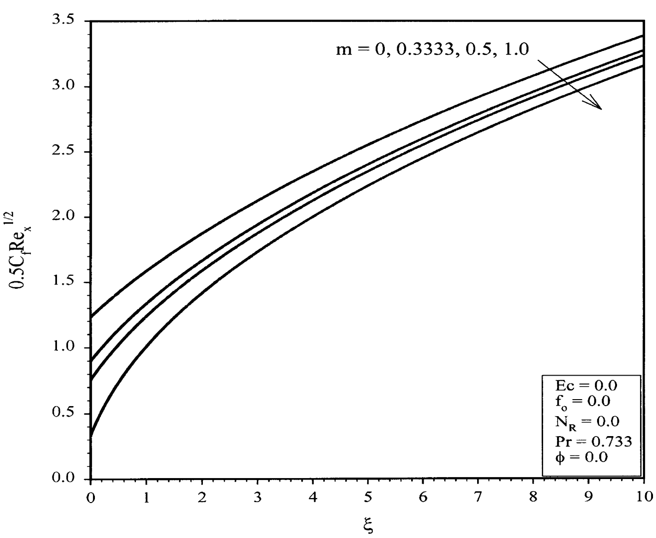

Fig. 7. Effects of m on Development of Skin-Friction Coefficient

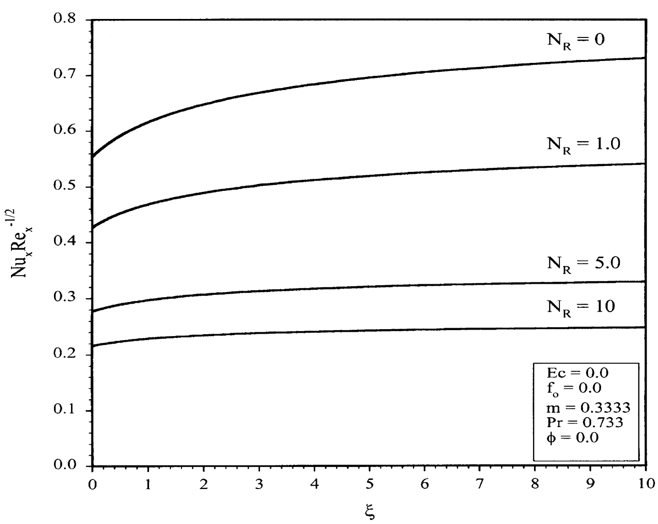

Fig. 10. Effects of N_R on Development of Nusselt Number

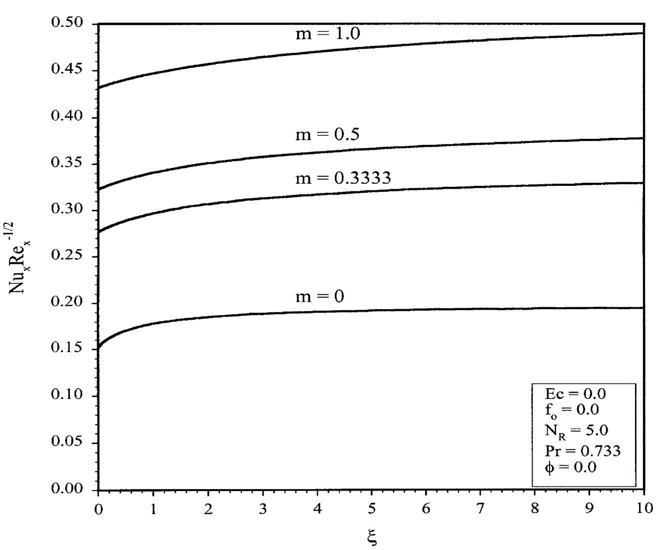

Fig. 8. Effects of m on Development of Nusselt Number

increases as N_R increases, the local Nusselt number decreases because it is proportional to the negative value of the wall slope of the temperature profile.

Figures 11a, 11b and 12 illustrate the changes that are brought about in the temperature profiles at ξ=1.0 and ξ=3.0 and the local Nusselt number due to changes in the values of the dimensionless heat generation or absorption coefficient, respectively. The presence of a heat source within the flow has the tendency to increase the thermal state of the fluid. This is depicted by the increases in the temperature profile at every point away from the wedge surface as ϕ increases displayed in Figures 11a and 11b. On the contrary, the presence of a heat sink (ϕ<0) within the flow reduces the temperature of the fluid away from the wall as is obvious from Figures 11a and 11b. The increase of the heat-generation or absorption coefficient ϕ appear to have no effect on the thermal boundary-layer for ξ = 1.0 and the parametric values employed to produce Figure 11a. However, it tends to increase it for ξ = 3.0 and the same parametric values. It is also observed from this

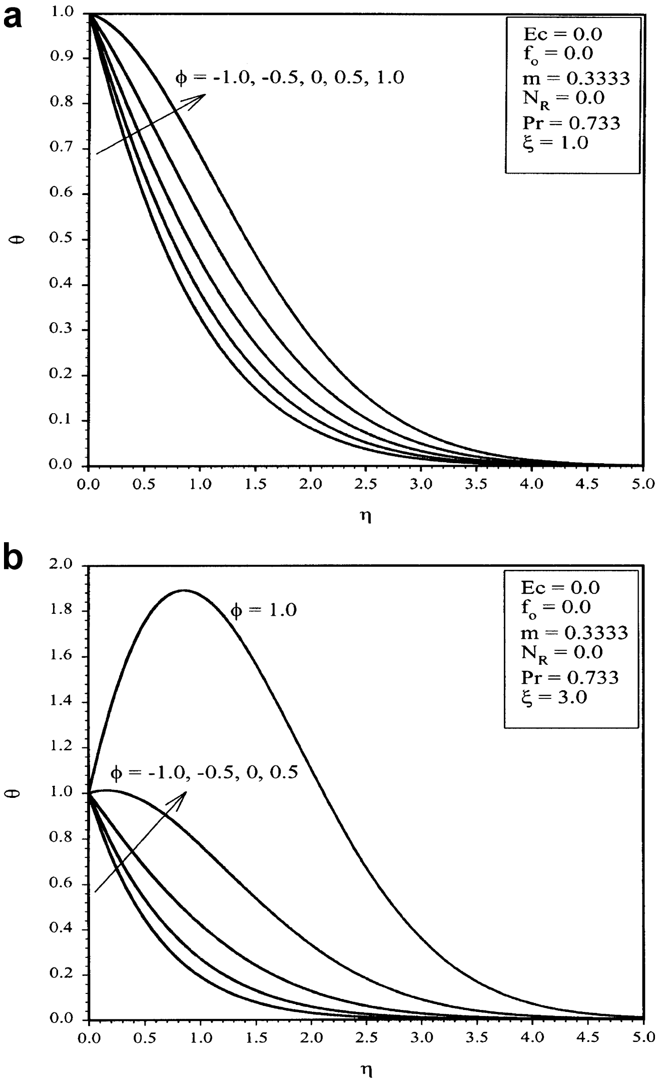

Fig. 11a, b. Effects of ϕ on Temperature Profiles

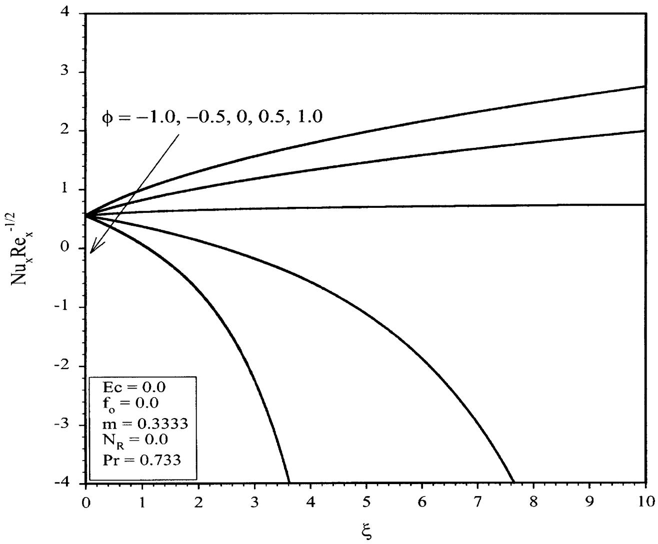

Fig. 12. Effects of ϕ on Development of Nusselt Number

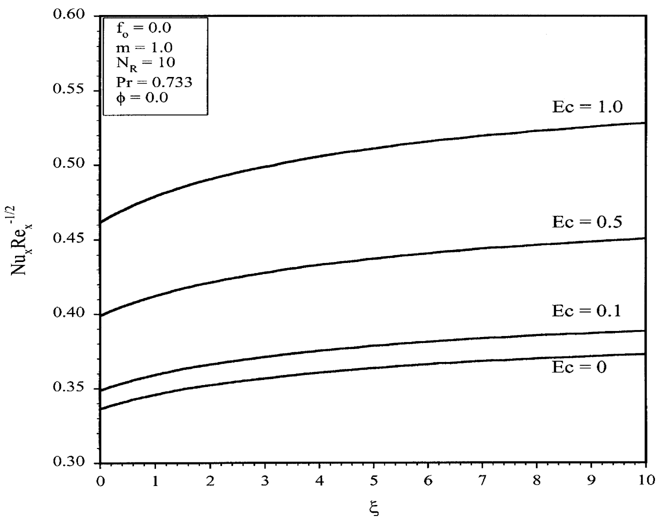

Fig. 13. Effects of Ec on Development of Nusselt Number

figure that the negative of the wall slope of the temperature profile at ξ=1.0 increases as the coefficient ϕ is reduced. This means that heat absorption (ϕ<0) causes enhancements in the local Nusselt number while heat generation (ϕ>0) reduces it as evident from Figure 12. It can also be observed from Figure 12 that for ϕ>0 the local Nusselt number becomes negative beyond certain values of ξ ($\xi \cong 3.0$ for ϕ = 0.5 and $\xi \cong 1.5$ for ϕ = 1.0). This means that the temperature profile at these values exhibits a peak value adjacent to the wall. This peak value is higher than that of the wall and, therefore, the wall heat transfer process is reversed. This is clearly seen from Figure 11b.

All of the above graphical results were produced for Ec = 0. Figure 13 shows the effects of the Eckert number Ec which represents the viscous and magnetic dissipations and stress work effects on the local Nusselt number in the presence of thermal radiation effects. It was shown by Yih (1999) that in the absence of thermal radiation effects (N_R = 0), the local Nusselt number reduces as Ec increases. However, in the presence of thermal radiation (N_R =10), Figure 13 suggests the contrary. That is, the local Nusselt number increases as viscous and magnetic dissipations and stress work effects become significant for all values of ξ.

5
Conclusion

The problem of steady, laminar, hydromagnetic forced convection boundary-layer flow over a non-isothermal wedge with permeable surface in the presence of thermal radiation and heat generation or absorption effects was considered. A transformed set of non-similar equations was obtained. These equations were solved numerically by the implicit finite-difference methodology. Favorable comparisons with various previously published special cases of the problem were performed. Results for the velocity and temperature profiles as well as the local skin-friction coefficient and local Nusselt number were presented for various parametric conditions. It was found that both the local skin-friction coefficient and local

Nusselt number increased as the wall mass transfer parameter was increased. In general, both the local skin friction coefficient and the local Nusselt number increased with increases in the strength of magnetic field as long as the wall mass transfer parameter is greater than or equal to zero. Also the local skin-friction coefficient was found to decrease while the local Nusselt number was found to increase as the free stream velocity (or pressure gradient) parameter was increased. In addition, the local Nusselt number was predicted to decrease as the thermal radiation parameter was increased. Furthermore, heat generation was found to decrease the local Nusselt number while heat absorption was found to increase it. Moreover, it was predicted that the presence of viscous and magnetic dissipations as well as stress work effects increased the local Nusselt number as long as thermal radiation effects were present.

References

Ariel, P.D., Hiemenz Flow in Hydromagnetics. Acta Mech., 1994, 103, 31–43

Blottner, F.G., Finite-Difference Methods of Solution of the Boundary Layer Equations. AIAA Journal, 1970, 8, 193–205

Cebeci, T. and Bradshaw, P., Physical and Computational Aspects of Convective Heat Transfer, 1st ed., p. 385. Springer-Verlag, New York, 1984

Chamkha, A.J., Hydromagnetic Natural Convection From an Isothermal Inclined Surface Adjacent to a Thermally Stratified Porous Medium, Int. J. Engrng Sci., 1997a, 35, 975–986

Chamkha, A.J., Non-Darcy Fully Developed Mixed Convection in a Porous Medium Channel with Heat Generation/Absorption and Hydromagnetic Effects, Numer. Heat Transfer, 1997b, 32, 853–875

Cramer, K. R. and Pai, S. I., Magnetofluid Dynamics for Engineers and Applied Physicists, Scripta Publishing Company, Washington D.C., 1973

Crepeau, J. C. and Clarksean, R., Similarity Solutions of Natural Convection with Internal Heat Generation. Journal of Heat Transfer, 1997, 119, 183–185

Fumizawa, M., Natural Convection Experiment With Liquid NaK under Transverse Magnetic Field, J. Nuclear Science and Technology, 1980, 17, 10–17

Gray, D.D., The Laminar Wall Plume in a Transverse Magnetic Field. Int. Commun. Heat Mass Transfer, 1979, 22, 1155–1158

Lin, H. T. and Lin, L. K., Similarity Solutions for Laminar Forced Convection Heat Transfer from Wedges to Fluids of any Prandtl Number. Int. J. Heat Mass Transfer, 1987, 30, 1111–1117

Michiyoshi, I., Takahashi, I. and Serizawa, A., Natural Convection Heat Transfer from a Horizontal Cylinder to Mercury Under Magnetic Field. Int. J. Heat Mass Transfer, 1976, 19, 1021–1029

Moalem, D., Steady State Heat Transfer with Porous Medium with Temperature Dependent Heat Generation. Int. J. Heat Mass Transfer, 1976, 19, 529

Raptis, A., "Flow of a Micropolar Fluid Past a Continuously Moving Plate by the Presence of Radiation". Int. J. Heat Mass Transfer, 1998a, 41, 2865–2866

Raptis, A., "Radiation and Free Convection Flow Through a Porous Medium". Int. Commun. Heat Mass Transfer, 1998b, 25, 289–295

Sparrow, E. M. and Cess, R. D., Temperature Dependent Heat Sources or Sinks in a Stagnation Point Flow, Appl. Sci. Res., 1961, A10, 185

Sparrow, E. M., Eckert, E. R., and Minkowycz, W. J., Appl. Sci. Res., 11, 1962, 125

Vajravelu, K. and Nayfeh, J., Hydromagnetic Convection at a Cone and a Wedge. Int. Commun. Heat Mass Transfer, 1992, 19, 701–710

Vajravelu, K. and Hadjinicolaou, A., Heat Transfer in a Viscous Fluid over a Stretching, Sheet with Viscous Dissipation and Internal Heat Generation. Int. Commun. Heat Mass Transfer, 1993, 20, 417–430

Watanabe, T. and Pop, I., Thermal Boundary Layers in Magnetohydrodynamic flow over a Flat Plate in the Presence of a Transverse Magnetic Field, Acta Mech., 1994, 105, 233–238

Westphal, B. R., Keiser, D. D., Rigg, R. H., and Lang, D. V., Production of Metal Waste Forms from Spent Nuclear Fuel Treatment, DOE Spent Nuclear Fuel Conference, Salt Lake City, UT, 1994, pp 288–294

Yih, K. A., MHD Forced Convection Flow Adjacent to a Non-Isothermal Wedge. Int. Comm. Heat Mass Transfer, 1999, 26, 819–827